The Lichenologist **46**(1): 103–114 (2014)
doi:10.1017/S002428291300073X

Phylogenetic position of the crustose *Stereocaulon* species

Filip HÖGNABBA, Raquel PINO-BODAS, Anders NORDIN, Leena MYLLYS and Soili STENROOS

Abstract: Phylogenetic relationships of *Stereocaulon* with emphasis on the crustose taxa were studied based on nuclear ribosomal ITS1–5.8S–ITS2 and partial beta-tubulin sequences. The placement of four of the six crustose species currently included in the genus has previously been confirmed based on molecular data. It has, however, remained unresolved whether the crustose growth form is a plesiomorphic or apomorphic feature within *Stereocaulon*, due to contradictory placements of the crustose species in earlier studies. The aim of this study was to clarify the position of the crustose species by including additional data, especially of *S. nivale* and *S. plicatile*, which have not been included in previous analyses. The inclusion of *S. plicatile* in the genus is of particular interest as it is the only species in the genus with submurifrom to muriform ascospores. Altogether 37 specimens representing 31 species of the ingroup, including all the crustose *Stereocaulon* species, were incorporated in the analyses. Conventional, as well as direct optimization parsimony, maximum likelihood and Bayesian analyses were performed. The results show that the crustose species do not form a monophyletic entity and that the crustose growth form is a plesiomorphic feature within *Stereocaulon*. The crustose *S. nivale* and *S. plicatile* are nested within the genus and their inclusion in *Stereocaulon* is thereby confirmed. The nested position of *S. plicatile* indicates that the submuriform to muriform spore type has been gained independently within the genus. Here, *S. plicatile* is also reported for the first time from Scandinavia.

Key words: ascospores, direct optimization, lichens, molecular phylogeny, muriform, submuriform

Accepted for publication 5 *September* 2013

Introduction

Species traditionally included in the genus *Stereocaulon* (*Stereocaulaceae*, lichenized Ascomycota) are characterized by a crustose primary thallus and a fruticose secondary thallus. The primary thallus consists of granules or squamules and is tightly attached to the substratum. The secondary thallus arises from the crustose primary thallus by elongation of thalline tissue and forms so-called pseudopodetia that support phyllocladia or phyllocladoid branchlets, apothecia and in most species cephalodia (Lamb 1951).

In addition to the species forming a dimorphic thallus, six crustose species completely lacking a secondary thallus are included in *Stereocaulon*. These species are *S. cumulatum* (Sommerf.) Timdal, *S. leucophaeopsis* (Nyl.) P. James & Purvis, *S. nivale* (Follmann) Fryday, *S. plicatile* (Leight.) Fryday & Coppins, *S. tornense* (H. Magn.) P. James & Purvis and *S. urceolatum* (P. M. Jørg.) Högnabba. With the exception of *S. urceolatum*, the crustose species were transferred to *Stereocaulon* based on morphological, anatomical and chemical characters (Purvis & James 1985; Fryday & Coppins 1996; Timdal 2002; Fryday & Glew 2003). The placement of *S. cumulatum*, *S. leucophaeopsis* and *S. tornense* in *Stereocaulon* has subsequently been confirmed based on molecular studies (Myllys *et al.* 2005; Högnabba 2006; see also Printzen & Kantvilas

F. Högnabba, R. Pino-Bodas, A. Nordin, L. Myllys and S. Stenroos (corresponding author): Botanical Museum, Finnish Museum of Natural History, P.O. Box 7, FI-00014 University of Helsinki, Finland.
Email: soili.stenroos@helsinki.fi
R. Pino-Bodas: Departamento Biología Vegetal 1, Facultad de Biología, Universidad Complutense de Madrid, 28040 Madrid, Spain.
A. Nordin: Museum of Evolution, Uppsala University, Norbyvägen 16, SE-75236 Uppsala, Sweden.

2004). Furthermore, *S. urceolatum* was first placed in the monotypic genus *Muhria* in the family *Stereocaulaceae* by Jørgensen & Jahns (1987). They had also considered inclusion of the species in *Stereocaulon* as it has so many characters in common with the genus. However, as the hemiangiocarpic apothecial ontogeny of the species is fundamentally different from the gymnocarpic apothecial ontogeny normally found in *Stereocaulon*, they concluded that a new genus to accommodate the species was needed. Molecular studies have, however, revealed that the species should be included in *Stereocaulon* (Myllys *et al.* 2005; Högnabba 2006; see also Ekman & Tønsberg 2002; Printzen & Kantvilas 2004). Hemiangiocarpic apothecial development has also been reported to occur in *S. cumulatum* and *S. tomentosum* (Timdal 2002), and occasionally in *S. dactylophyllum* (Jahns 1970).

Stereocaulon plicatile is a crustose and sorediate species with *Porpidia*-type asci and submuriform to muriform ascospores. Fryday & Coppins (1996) mention that, apart from the ascospores, *S. plicatile* is almost impossible to distinguish from *S. tornense*, but based on the material examined they concluded that *S. plicatile* tends to have a thinner and less well-developed thallus with more dispersed and flatter areoles. A detailed description of the species is provided by Fryday & Coppins (1996). The species has so far been reported only from the British Isles, where it occurs in montane areas mostly above 800 metres, and from Maine, North America (Fryday 2006). Fryday & Coppins (1996), however, note that it is almost certainly present in other mountainous areas and that it should be looked for particularly in Scandinavia. The inclusion of *S. plicatile* in the genus is interesting as it is the only species in the genus with submuriform to muriform ascospores. Normally, the species in *Stereocaulon* have transversely septate ascospores (Lamb 1977; Timdal 2002), although Lamb (1977) observed that spores may rarely have one to two longitudinal septa.

The phylogenetic position of the crustose species within *Stereocaulon* is still unresolved. In Myllys *et al.* (2005), the crustose *S. tornense* appears as the basal taxon of *Stereocaulon*, forming the sister taxon to the rest of the genus. The clade including all *Stereocaulon* species sampled except *S. tornense* was further divided into two major monophyletic groups, one of which included the remaining crustose species and the other all the fruticose species included in that study. In Högnabba (2006), on the other hand, the crustose species formed a monophyletic group that was well nested within *Stereocaulon*, with the exception of one of the two included specimens of *S. cumulatum* that appeared as the sister taxon to a clade consisting of all the *Stereocaulon* specimens included, except the basal *S. sorediiferum*. The results in Myllys *et al.* (2005) indicate that the crustose growth form is a plesiomorphy, while the results in Högnabba (2006) suggest that the crustose growth form is an apomorphic feature within *Stereocaulon*.

In order to resolve this ambiguity and to reconsider the phylogenetic position of the species with crustose growth form, we here include two additional crustose species, *S. nivale* and *S. plicatile*, in DNA sequence analyses. In the light of the phylogenetic hypotheses obtained, we discuss the evolution of the crustose growth form and the submuriform/muriform spore type. In addition, *S. plicatile* is reported for the first time from Scandinavia, and its morphological variation is discussed.

Material and Methods

Morphology and chemistry

The morphology of the *S. plicatile* material from Sweden was studied using standard light microscope techniques. Spore measurements were made on material mounted in water. Extrolites were detected using thin-layer chromatography (TLC) as described in Orange *et al.* (2001).

DNA extractions, amplification and sequencing

Total DNA was extracted using DNeasy® Plant Mini Kit (Qiagen) or DNeasy® Blood and Tissue Kit (Qiagen) according to the protocols enclosed with the kits, except that the liquid nitrogen phase was omitted for both kits. Instead, the thallus fragments were ground with a mini-pestle in a small amount of lysis buffer provided with the

kits. The DNA extracted was eluted in 160 µl of elution buffer when the Plant Mini Kit was used, and 100 µl of elution buffer when the Blood and Tissue Kit was used. The extraction products were used undiluted in the PCR reactions.

To amplify the nITS rDNA region, the primer pairs ITS1F (Gardes & Bruns 1993) and ITS4 (White *et al.* 1990) or ITS1-LM (Myllys *et al.* 1999) and ITS2-KL (Lohtander *et al.* 1998) were used. The partial beta-tubulin gene was amplified using the primer pair Bt3-LM and Bt10-LM (Myllys *et al.* 2001). PCR amplification was undertaken using illustra PuReTaq Ready-To-Go™ PCR Beads (GE Healthcare). The 25 µl PCR samples were prepared by adding 1 µl of each primer at 10 µM concentration, 4 or 5 µl of template DNA and 18–19 µl sterile water to the 0·2 ml tubes with PCR beads. PTC-100, PTC-200 Thermal Cyclers (MJ Research) and Mastercycler® ep gradient S (Eppendorf) were used to perform the PCR cycles. Slightly different settings were successfully used in the PCR reactions. ITS1F+ITS4: 95°C for 5 min; 5 cycles of 30 s at 95°C, 30 s at 55°C, 60 s at 72°C; 30 cycles of 30 s at 95°C, 30 s at 52 or 53°C, 60 s at 72°C; 7 min at 72°C (omitted for some of the reactions). ITS1F+ITS4 and ITS1L-M+ITS2KL: 95°C for 5 min; 5 cycles of 30 s at 95°C, 30 s at 58°C, 60 s at 72°C; 30 cycles of 30 s at 95°C, 30 s at 56°C, 60 s at 72°C; 7 min at 72°C; Bt3-LM+Bt10-LM: 95°C for 5 min; 5 cycles of 30 s at 95°C, 30 s at 55 or 56°C, 60 s at 72°C; 30 cycles of 30 s at 95°C, 30 s at 52 or 54°C, 60 s at 72°C; 7 min at 72°C. The PCR products were purified using illustra GFX PCR DNA and Gel Band Purification Kit (GE Healthcare) following the manufacturer's instructions. Purified DNA was eluted with 30–50 µl sterile water (elution buffer 6) included in the kit. The amount of sterile water used depended on the strength of the product when visually observed on an agarose gel.

For sequencing of the PCR products, BigDye® Terminator v1.1 Cycle Sequencing Kit (Applied Biosystems) was used. Sequencing samples containing 3 µl BigDye, 1 µl primer at 2·5 µM concentration, 2 µl purified PCR product and 4 µl sterile water were prepared. The primers used for sequencing were the same as listed above for the PCR amplification. The samples were run using the following settings: 96°C for 30 s, 50°C for 15 s, and 60°C for 4 min. The same equipment as in the PCR reactions was used to run the sequencing reactions. For the post-reaction purification of the samples, the protocol described in Högnabba (2006) was followed. Sequencing of these samples was made by an ABI prism 377 automatic sequencer. Sequencing of the remaining samples was carried out at Macrogen Inc. (http://www.macrogen.com). The DNA concentration of the PCR products sequenced at Macrogen was measured using a BioPhotometer (Eppendorf) and UVette® cuvettes (Eppendorf) using the 10 mm optical path length. 50 µl dilutions of the PCR products were prepared for the concentration measurements by adding 7 µl of the PCR products and 43 µl sterile water.

SeqMan II version 4.0 (DNASTAR) was used to assemble the sequences obtained. IUPAC ambiguity codes were used when base calling was equivocal. BLAST searches were used to confirm the sequence identity. All the new sequences were homologous (>94% of identity) with *Stereocaulon* sequences in GenBank.

Taxon sampling

To study the position of the crustose species of *Stereocaulon*, a dataset based on that published in Högnabba (2006) was constructed. Representatives from all the major groups recognized in that study were selected (Table 1). Of the fruticose species, only specimens where both ITS and beta-tubulin sequences were available were selected, with the exception of *S. sorediiferum* which was the basal taxon of the genus in Högnabba (2006), forming the sister group to the rest of the genus. For this taxon, only the beta-tubulin sequence was available despite several attempts to sequence the ITS regions. The ITS sequence of *S. delisei* was newly sequenced for this study. For the crustose members of the genus, all sequences available were included in the analyses. Sequences of *S. nivale* (two specimens) and *S. plicatile* were produced for the first time for this study. In addition, the beta-tubulin sequence of one new *S. leucophaeopsis* specimen was included, and the ITS region was successfully sequenced for one of the *S. urceolatum* specimens for which only the beta-tubulin sequence was included in Högnabba (2006). Altogether, eight new sequences of the crustose *Stereocaulon* specimens were included in this study. Species from the genus *Lepraria* were selected as outgroup taxa. The genus *Lepraria* is included in the family *Stereocaulaceae* (Lumbsch & Huhndorf 2010) and has been shown to form the sister group of *Stereocaulon* (Myllys *et al.* 2005; Miądlikowska *et al.* 2006). We also made preliminary analyses including more distantly related taxa from the *Cladoniaceae* and the *Lecanoraceae*. In all analyses, *Lepraria* and *Stereocaulon* formed a sister group. In the final analyses we therefore chose to include only *Lepraria* as outgroup due to alignment problems of the ITS regions when more distantly related taxa were included. The final dataset consisted of 37 specimens of 31 species from the ingroup, including all crustose species currently classified in *Stereocaulon*. Three specimens representing two taxa of the outgroup were included in the final analyses.

Sequence alignment and phylogenetic analyses

We used four different approaches for analyzing the data: conventional parsimony, parsimony with direct optimization, maximun likelihood (ML) and Bayesian inference. In the conventional parsimony approach, ML and the Bayesian methods, the sequences were aligned prior to the analyses. The ITS regions showed considerable length variation and the included beta-tubulin intron region showed minor length variation. Alignments (available by contacting the corresponding author) of these regions were made with the software MUSCLE version 3.7 (Edgar 2004). Ambiguously aligned sites of the ITS regions were removed manually. The 5.8S region that was aligned together with the ITS regions showed no length variation. The exons of the beta-tubulin sequences were all of equal length and could be

TABLE 1. *Specimen information and GenBank accession numbers for sequences of* Stereocaulon *and outgroup species analyzed in this study. New sequences are indicated by accession numbers in bold.*

Taxon name	Voucher	Extraction code	GenBank Accession Number	
			ITS	beta-tubulin
Lepraria jackii	Finland, *Myllys & Lohtander* 273 (TUR)	–	KF682450	DQ099615
L. jackii	Finland, *Myllys & Lohtander* 286 (TUR)	–	KF682451	DQ099618
L. membranacea	Finland, *Myllys & Lohtander* 272 (TUR)	–	KF682452	DQ099622
Stereocaulon alpinum	Argentina, *Stenroos* 5496 (TUR)	AT1077	DQ396917	DQ396995
S. azoreum	Madeira, *Krebs* 5175 (B)	FH56	DQ396966	DQ397036
S. coniophyllum	China, Tibet, *Obermayer* 8635 sorediate (GZU)	AT1144	DQ396937	DQ397012
S. corticatulum	Argentina, *Stenroos* 5403 (TUR)	AT1047	DQ396904	DQ396983
S. cumulatum	Norway, *Haugan* SK00-114 (O)	FH7	KF682458	DQ099628
S. cumulatum	Norway, *Timdal* 9132 (O)	FH8	DQ396963	–
S. curtatum	Japan, *Inoue* 28955 (TUR)	AT1167	DQ396949	DQ397023
S. delisei	Norway, *Högnabba* 558 (H)	FH69	KF682457	DQ397046
S. exutum	Japan, *Inoue* 28958 (TUR)	AT1165	DQ396948	DQ397022
S. foliolosum	China, Tibet, *Obermayer* 8645 (GZU)	AT1138	DQ396933	DQ397008
S. fronduliferum	New Zealand, Vězda Lich. rar. exs. 279 (H)	FH6	DQ396962	DQ397033
S. glabrum	Argentina, *Stenroos* 5460 (TUR)	AT1054	DQ396906	DQ396985
S. intermedium	China, Tibet, *Obermayer* 8634 granulose (GZU)	AT1142	DQ396935	DQ397010
S. japonicum	Korea, *Inoue* 28951 (TUR)	AT1162	DQ396945	DQ397019
S. leucophaeopsis	Norway, *Timdal* 9636 (O)	FH72	DQ396971	–
S. leucophaeopsis	Sweden, *Nordin* 6515 (UPS)	FH239	KF682453	–
S. myriocarpum	China, Tibet, *Obermayer* 8202 (GZU)	AT1133	DQ396931	DQ397006
S. nanodes	Norway, *Løfall* bpl-L 9587 (O)	FH71	DQ396970	DQ397048
S. nivale	USA, Washington, *Glew* 020928-1 (WTU)	FH125	KF682456	KF682459
S. nivale	USA, Washington, *Glew* 020928-3 (H)	FH126	KF682455	KF682460
S. paschale	Finland, *Ahti* 60905 (H)	AT1035	DQ396897	DQ396977
S. pendulum	Japan, *Högnabba* 247 (H)	FH64	DQ396969	DQ397041
S. plicatile	Sweden, *Nordin* 6510 (UPS)	FH238	KF682454	KF682461
S. ramulosum	Hawai'i, *Inoue* 27242 (TUR)	AT1160	DQ396944	DQ099629
S. rivulorum	Norway, *Sipman* 44112 (B)	FH60	DQ396967	DQ397038
S. sasakii	Japan, *Sasaki* 13825 (TUR)	AT1187	DQ396958	DQ397031
S. saxatile	Finland, *Stenroos* 5591 (TUR)	AT1078	DQ396918	DQ396996
S. saxatile	Finland, *Stenroos* 5603 (TUR)	AT1090	DQ396927	DQ397004
S. sorediiferum	Japan, *Högnabba* 341 (H)	FH63	–	DQ397040
S. taeniarum	Finland, *Stenroos* 5593 (TUR)	AT1080	DQ396919	DQ397053
S. tomentosum	Finland, *Ahti* 60910 (H)	AT1032	DQ396894	DQ099631
S. tornense	Norway, *Dahlkild* s. n. (H)	FH78	DQ396975	DQ099632
S. urceolatum	Sweden, *Muhr* s. n. (TUR)	AT1192	–	DQ099623
S. urceolatum	Sweden, *Muhr* s. n. (TUR)	AT1193	DQ396959	DQ099624
S. urceolatum	Not available	–	AF517926	–
S. verruciferum	Argentina, *Stenroos* 5289 (TUR)	AT1037	DQ396899	DQ099633
S. vesuvianum	Finland, *Stenroos* 5599 (TUR)	AT1088	DQ396925	DQ397002

aligned manually without problems. In order to examine putative conflicts among the loci, bootstrap analysis of the alignment of ITS regions and beta-tubulin separately was carried out. Each clade with bootstrap support >75% was scanned, according to the method described by Lutzoni *et al.* (2004). No conflicts were found and the alignments were concatenated. The conventional parsimony analysis was made with the program TNT (Goloboff *et al.* 2008). A traditional search with the following settings was performed: starting trees obtained

with 1000 replicates, TBR branch-swapping algorithm, saving 20 trees per replicate, gaps were treated as a 5th character state. Jackknife support values (Farris *et al.* 1996) for the nodes were calculated with 1000 replicates using the program TNT.

Length variation in the non-coding regions such as the ITS often causes problems with homology assumptions, and alignments of such regions often include ambiguously aligned sites. To overcome the alignment problems caused by the length variation in the ITS regions and the beta-tubulin intron region, we performed direct optimization (Wheeler 1996) as an alternative to the conventional parsimony approach. In the direct optimization procedure the homology assumptions and the tree search are made simultaneously, without the need to align the sequence prior to analysis. In the analyses, direct optimization was performed for the ITS and the beta-tubulin intron regions, while the 5.8S region and the beta-tubulin exon regions were treated as prealigned (i.e., left as fixed alignments within this analysis). The analysis was performed using version 1.4.2.1 of the program POY (Varón *et al.* 2008, 2010) running on the Vuori HP CP4000 BL ProLiant supercluster at the IT Center for Science, Espoo, Finland. Initially, 1000 random-addition trees were generated with transitions, transversions, and indels given equal weight. The initial trees were refined using SPR and TBR branch swapping. In addition to the optimal trees, suboptimal trees up to 10% longer than the optimal trees were evaluated during the SPR and TBR swapping. This was followed by 15 rounds of ratcheting (Nixon 1999) in which 20% of the characters were re-weighted randomly by a factor of three. Finally, 200 iterations of tree-fusing (Goloboff 1999) were performed. All optimal and unique trees were retained between the different searches. The commands used in the POY analysis are provided in Appendix 1. For each of the most parsimonious trees found, separate implied alignments of the regions subjected to direct optimization were obtained. The implied alignments were concatenated with the alignments of the regions without length variation using the program MacClade (version 4.06; Maddison & Maddison 2003). The matrices obtained were used for calculating jackknife support values (Farris *et al.* 1996) for the clades. Separate jackknife analyses were run for each matrix. If the analyses resulted in different support for a clade, the lowest and highest values are indicated. The jackknife support values were calculated in 1000 replicates using the program TNT (Goloboff *et al.* 2008).

The strict consensus of the most parsimonious trees retained in the conventional parsimony analysis was calculated using the software Mesquite version 2.74 (Maddison & Maddison 2010). In the direct optimization analysis, the strict consensus of the retained trees was exported at the end of the POY analysis.

We used maximum likelihood analysis as implemented in RAxML 7.04 (Stamatakis 2006), using GTRGAMMA model with four partitions (ITS and each codon position of beta-tubulin). All the parameters were estimated from the data. The clade support was estimated with 500 replicates of 'fast bootstrap'. Bayesian analysis was carried out in MrBayes 3.1.2 (Huelsenbeck & Ronquist 2001) with default priors. The best-fit evolutionary model to each loci was selected by MrModeltest (Nylander 2004) under AIC criterion. The GTR+G and GTR+I+G models were selected for beta-tubulin and ITS regions, respectively. The posterior probabilities were approximated by sampling trees using Markov Chain Monte Carlo (MCMC). Two simultaneous runs with 10 000 000 generations, each starting with a random tree and employing 4 simultaneous chains, were executed. Every 1000th tree was saved into a file. The convergence of the chains was determined with TRACER 1.5 (Rambaut & Drummond 2007) and a standard deviation of split frequencies was $<0{\cdot}005$ between the runs. The potential scale reduction factor (PSRF) was 1·0 for all the parameters. The first 1 000 000 generations were deleted as the 'burn in' of the chain and the 50% majority-rule consensus tree was calculated using the 'sumt' command in MrBayes.

The trees were visualized using the software FigTree version 1.3.1 (Rambaut 2009), and the graphical appearance of the trees shown was further edited using the program Inkscape version 0.47preI r21720 (http://www.inkscape.org).

Results

Stereocaulon plicatile (Leight.) Fryday & Coppins in Scandinavia

A crustose *Stereocaulon* species with submuriform to muriform spores was found by A. Nordin during fieldwork in Jämtland, Sweden in 2007. The species found in Jämtland contained atranorin and stictic acid and thereby has the same chemistry as reported for *S. plicatile*. Some of the other characteristics of the Swedish material, however, differ slightly to what was reported for *S. plicatile* by Fryday & Coppins (1996). The size of the ascospores of the Swedish material was found to be 22·6–[30·0]–35·0 × 9·0–[11·7]–14·7 µm (mean values in brackets, $n = 17$) compared to 20–32 × 10–15 µm reported for *S. plicatile*. The mean values of the length and width of the spores in the Swedish material, however, fall within the ranges reported for the species. The apothecia in the Swedish material are up to 3 mm wide while the apothecia in *S. plicatile* were reported to be up to 1·6 mm wide. Finally, the hymenium in the Swedish material seems to be thicker than 110 µm, as was mentioned in the species description of *S. plicatile*. The Swedish material was found in an old copper mine, whereas *S. plicatile* was reported to occur on

siliceous rocks and pebbles, and no possible copper association was mentioned. Cephalodia were reported to be absent in *S. plicatile*. However, the material collected in Sweden is associated with *Stigonema*. This kind of loose association with cyanobacteria (attached to the thallus, but not confined to cephalodia) is also reported for the other crustose *Stereocaulon* species (Jørgensen & Jahns 1987; Jahns *et al.* 1995; Timdal 2002). Furthermore, when compared to the material of *S. plicatile* collected by Fryday (no. 5609, UPS), the general appearance of the Swedish material is very similar. Interestingly, this specimen is also associated with *Stigonema*. In our opinion, it is unlikely that there are two crustose *Stereocaulon* species with submuriform to muriform spores and the same chemistry that would be morphologically so similar. Therefore, our conclusion is that the Swedish material belongs to *S. plicatile*, but the variation of some of the morphological characteristics is slightly wider than reported by Fryday & Coppins (1996), who actually stated that the species should particularly be looked for in Scandinavia. However, until molecular data from British material has been obtained for comparison, the relationship between the populations remains uncertain. The Scandinavian population probably extends to adjacent areas in Norway, and might even be distributed along the Scandinavian mountains further north and reach northern Finland.

Specimens examined. **Sweden:** *Jämtland*: Åre parish, Handöl copper mine just W of the road between Handöl and Storulvån, *c.* 1 km S of Handöl, 63°14′45·8″N, 12°25′47·3″E (WGS84), alt. 640 m, on rock in an open shaft close to the road, 2007, *A. Nordin* 6510 (UPS); on loose pieces of rock in the N-most open shaft, 2008, *A. Nordin* 6677 (UPS); on rockwall in the E-most open shaft, 2008, *A. Nordin* 6680 (UPS).—**Great Britain:** *Scotland*: **V.C. 97,** West Inverness-shire: Creag Meagaidh, Grid 27/405,871, alt. 1000 m, on siliceous pebbles above area of prolonged snow-lie, NW of summit, 1994, *A. M. Fryday* 5609 (UPS).

Phylogenetic analyses

The concatenated alignment contained 1210 positions (454 of ITS regions and 756 of beta-tubulin), of which 824 were constant (285 of ITS regions and 539 of beta-tubulin) and 276 were parsimony-informative (116 of ITS regions and 160 of beta-tubulin). The conventional phylogenetic analysis resulted in 78 equally parsimonious trees with a length of 952 steps. The direct optimization analysis resulted in four equally parsimonious solutions with a length of 1459 steps. The tree lengths from the analyses are not comparable as the ambiguously aligned sites were removed from the alignment before it was used in the conventional analysis, and therefore fewer characters were included. The strict consensus tree of the direct optimization analysis is somewhat more resolved than the strict consensus tree of the conventional phylogenetic analysis. However, in both phylogenies five major, highly supported clades can be recognized. These are: 1) *S. cumulatum* (jackknife = 100/100), 2) *S. urceolatum* (j = 99/99–100), 3) the crustose *Stereocaulon* species except *S. cumulatum* and *S. urceolatum* (j = 98/99–100), 4) subgenus *Holostelidium* (j = 85/89–91), and 5) subgenus *Stereocaulon* (j = 98/99–100). The clades and support values are indicated in the strict consensus of the trees found in the direct optimization analysis (Fig. 1). The results from the parsimony analyses are essentially the same and therefore we only show the direct optimization tree. The ML analyses yielded a tree with the likelihood value of LnL = −6059·93, while the likelihood for the Bayesian tree was LnL = −6327·26. The ML and Bayesian topology showed five well-supported clades similar to those in the parsimony analyses. Figure 2 shows the 50% majority-rule consensus tree of the Bayesian analysis.

The relationships between the major groups are identical in the results obtained from the four analyses, with the exception that *S. cumulatum* is the basal taxon of the genus in the strict consensus obtained from direct optimization, ML and Bayesian analyses, while in the strict consensus from the conventional parsimony analysis a trichotomy is formed at the base of *Stereocaulon*, leaving the basal taxon of the genus unresolved. In the clades comprising more than one species, the relationships between the species are identical in clade 4 in all analyses, while the phylogenetic

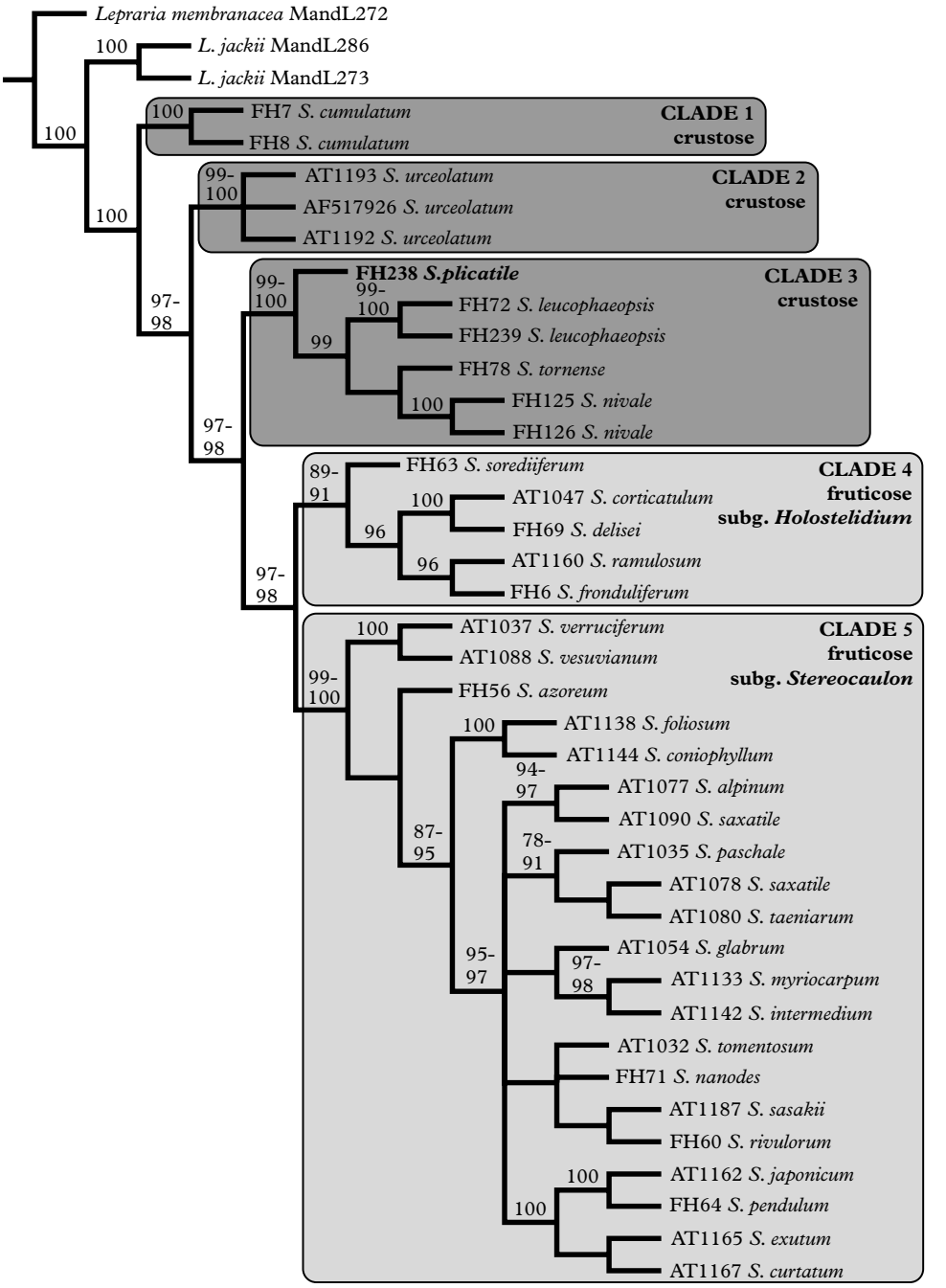

FIG. 1. Phylogenetic relationships among *Stereocaulon* species with emphasis on the crustose taxa. The strict consensus of four equally parsimonious trees for *Stereocaulon* species found in the direct optimization procedure. Jackknife support values are indicated above the nodes when ≥70. For the nodes where the support value differed between the four jackknife analyses, based on the different implied alignments, the highest and lowest supports obtained are indicated. Main clades, growth form, current classification for the fruticose species and extraction codes are indicated. The placement of *S. plicatile* with submuriform to muriform spores is indicated in bold.

https://doi.org/10.1017/S002428291300073X Published online by Cambridge University Press

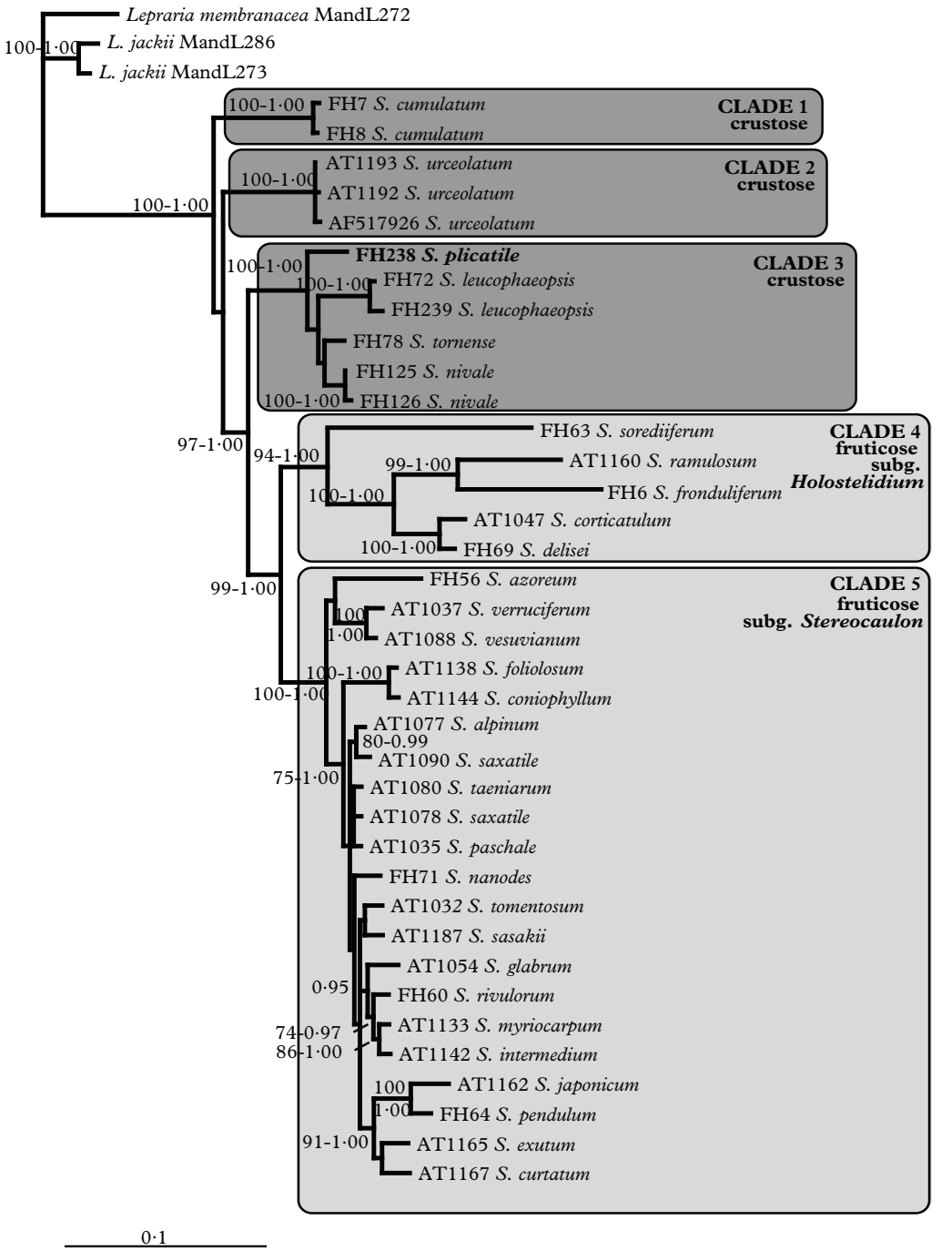

FIG. 2. Phylogenetic relationships among *Stereocaulon* species with emphasis on the crustose taxa. The 50% majority-rule consensus tree of a Bayesian analysis of nrITS and beta-tubulin of *Stereocaulon* species. Branch support is shown where bootstrap ≥70% for ML and posterior probability ≥0·95.

https://doi.org/10.1017/S002428291300073X Published online by Cambridge University Press

relationships within clades 3 and 5 differ to some extent between the trees. In clade 3, *S. plicatile* forms the basal taxon of the clade in all analyses. In the consensus tree of the conventional parsimony analysis, the relationships between *S. leucophaeopsis*, *S. nivale* and *S. tornense* are not resolved, while in the other analyses *S. leucophaeopsis* is the sister taxon to a group formed by *S. nivale* and *S. tornense*. Clade 5 is highly unresolved in the different analyses and the positions of some taxa differ between the analyses.

Discussion

Our results imply a basal position of the crustose *Stereocaulon* species in the genus and that the crustose species do not form a monophyletic entity. The basal position of the crustose species suggests that the crustose growth form is the plesiomorphic feature of the genus. Our results show that the crustose *S. plicatile* and *S. nivale*, which are incorporated in molecular analyses for the first time, are included in a strongly supported clade together with the crustose *S. leucophaeopsis* and *S. tornense*. Thus, the inclusion of these two taxa in the genus is also supported by DNA sequence data. The division of the subgenera *Holostelidium* and *Stereocaulon* into two clades supports the recognition of the two subgenera.

The basal position of the crustose species is supported by the conventional parsimony, the direct optimization, ML and Bayesian analyses. However, in the trees from the direct optimization, ML and Bayesian analyses, *S. cumulatum* is the basal taxon forming the sister species to the rest of the genus and *S. urceolatum* forms the sister taxon to the monophyletic group formed by the clades 3–5. In the conventional parsimony analysis, a trichotomy is formed at the base of the genus, and the relationship between *S. cumulatum* and *S. urceolatum*.

The basal position of crustose *Stereocaulon* species is in accordance with the results presented in Myllys *et al.* (2005). However, in that study, *S. tornense* formed the basal taxon of the genus. In the results presented here, *S. tornense* is nested in clade 3 together with the crustose *S. leucophaeopsis*, *S. nivale* and *S. plicatile*. In the combined analysis in Myllys *et al.* (2005), *S. cumulatum* and *S. urceolatum* (as *Muhria urceolata*) formed a clade with *S. leucophaeopsis*. This grouping is not observed in the present study. In Högnabba (2006), all the crustose *Stereocaulon* species, with the exception of one specimen of *S. cumulatum* (FH8), formed a clade that was nested within the genus. This relationship suggested that the crustose species formed a lineage in which the fruticose growth form has been lost, or is currently not expressed. Plausible explanations for the observed differences in the results of the previous and present studies are character and/or taxon sampling. In the present study, we included one intron region of the beta-tubulin sequences that was excluded in Myllys *et al.* (2005). The intron may have brought additional information to the analyses. Furthermore, in Myllys *et al.* (2005), the focus was on the family level and therefore the selection of loci was different (ITS not used). The loci used in the present study and in Högnabba (2006) are identical. The differences observed in the position of the crustose species are therefore most probably a result of the more extensive taxon sampling of the crustose species presented here. The absence of monophyly of *S. cumulatum* in Högnabba (2006) is probably due to stochastic errors in the analyses. The specimen of *S. cumulatum* (FH7) was represented only by the beta-tubulin sequence, and the other specimen of *S. cumulatum* (FH8) was represented only by the ITS sequence. In the present work, both specimens have ITS sequences and they are identical. Therefore, the current relationship is more robust than in the previous phylogenies. The crustose morphology was suggested to be the ancestral growth form in *Stereocaulon* by Lamb (1951). Assuming that Lamb's hypothesis was correct, Fryday & Glew (2003) suggested that *S. nivale* would occupy a basal position in *Stereocaulon*. Our results support the hypothesis postulated by Lamb (1951), but not the basal position of *S. nivale* as suggested by Fryday & Glew (2003).

The position of *S. plicatile* and *S. nivale* in clade 3 is supported by all analyses. The inclusion of these two crustose taxa in *Stereocaulon* that was based on morphological and chemical characters is thus clearly supported also by DNA sequence data, and their inclusion in *Stereocaulon* is thereby well founded. The inclusion of *S. plicatile*, with submuriform to muriform spores, is particularly interesting. The nested position of *S. plicatile* in *Stereocaulon* suggests that the submuriform to muriform spore type is an autapomorphic character that has been gained independently within the genus.

Timdal (2002) tabulated distinguishing features of the crustose *Stereocaulon* species, excluding *S. nivale* which was characterized and transferred to *Stereocaulon* later (Fryday & Glew 2003). Some of the features listed in these works separate clade 3 from the more basal *S. cumulatum* and *S. urceolatum*: the maximum areole diameter is 0·5–1·0 mm (vs. 4 and 5 mm for *S. cumulatum* and *S. urceolatum*, respectively), the apothecia are gymnocarpic (vs. hemiangiocarpic in the basal species), and the maximum apothecium diameter is 1·4–1·6 mm (vs. 0·5 mm in the basal species). In Scandinavian *S. plicatile*, the apothecia are even wider (see species description). Thus, the well-supported clade 3 can also be recognized based on morphological characters, which opens up the possibility of treating the group as a taxonomic entity, preferably as a subgenus. Furthermore, *S. cumulatum* and *S. urceolatum* that form clades 1 and 2, respectively, should then be included in separate monotypic subgenera. However, this taxonomic treatment is not done here. The few studies including crustose *Stereocaulon* species are in contradiction (see above) and further studies including additional data, more loci in particular, are necessary to reach phylogenetic stability, based on which well-founded taxonomic decisions can be made. Also, inclusion of additional fruticose taxa, especially of the subgenus *Holostelidium*, which are under-represented in the analyses published so far, is necessary.

The fruticose species form two major clades. Clade 4 corresponds to the subgenus *Holostelidium* and clade 5 to the subgenus *Stereocaulon*. This result is essentially in accordance with the results in Högnabba (2006), where the subgenus *Holostelidium* formed a monophyletic group with the exception of *S. sorediiferum*, which was the basal species of the genus. Also in that analysis, the subgenus *Stereocaulon* was monophyletic with the exception of *S. pileatum*, *S. virgatum* and one specimen of *S. verruciferum*. This can be explained by the fact that, for these three specimens only, the ITS regions were included in the analyses presented in Högnabba (2006). One specimen of *S. verruciferum*, for which the beta-tubulin sequence was also included, was clearly nested in the subgenus *Stereocaulon*.

The subgenus *Holostelidium* is characterized by the so-called holostelidious pseudopodetia development, in which the pseudopodetia are formed by elongation of all layers of the primary thallus. In the subgenus *Stereocaulon*, the pseudopodetia are formed by elongation of the basal medullary layer of the primary thallus (i.e. enteropodious pseudopodetia development). As the two subgenera form distinct groups, the pseudopodetia development seems to be a good feature with which to separate them. This is perhaps not a surprise as the two types of pseudopodetia development are essentially different (Lamb 1951).

Within the subgenus *Holostelidium*, the relationships between the species are identical in all analyses. Also, the relationships within subgenus *Holostelidium* found in the present study are in accordance with the results in Högnabba (2006), with the exception of *S. sorediiferum* as mentioned above. The contradictory placement of *S. sorediiferum* needs further investigation. Interestingly, *S. sorediiferum* is included in the section *Holostelidium*, while all other species of the subgenus *Holostelidium* included here, as well as in Högnabba (2006), are placed in the section *Aciculisporae* by Lamb (1977). Within the subgenus *Stereocaulon*, the relationships between the taxa differ between the conventional and the direct optimization methods. This may be because ambiguously aligned sites were discarded prior to the conventional analyses. The clades found within the

subgenus *Stereocaulon* in the direct optimization tree correspond in most cases to clades found within the corresponding group in Högnabba (2006). However, to reach final conclusions about phylogenetic relationships of the fruticose species, further studies including broader sampling of taxa and loci are required.

We thank P. Tahvanainen and M. Piisilä for assistance in the laboratory, J. Hyvönen for valuable advice on the phylogenetic analyses and T. Ahti for comments on the manuscript. LM and SS were supported by the Academy of Finland (grants 133858, 211172, 124203) and FH by the Oskar Öflund Foundation. The Willi Hennig Society is acknowledged for making the program TNT freely available.

References

Edgar, R. C. (2004) MUSCLE: multiple sequence alignment with high accuracy and high throughput. *Nucleic Acids Research* **32:** 1792–1797.

Ekman, S. & Tønsberg, T. (2002) Most species of *Lepraria* and *Leproloma* form a monophyletic group closely related to *Stereocaulon*. *Mycological Research* **106:** 1262–1276.

Farris, J. S., Albert, V. A., Källersjö, M., Lipscomb, D. & Kluge, A. G. (1996) Parsimony jackknifing outperforms neighbor-joining. *Cladistics* **12:** 99–124.

Fryday, A. M. (2006) New and interesting North American lichen records from the alpine and sub-alpine zones of Mt. Katahdin, Maine. *Bryologist* **109:** 570–578.

Fryday, A. M. & Coppins, B. J. (1996) A new crustose *Stereocaulon* from the mountains of Scotland and Wales. *Lichenologist* **28:** 513–519.

Fryday, A. M. & Glew, K. A. (2003) *Stereocaulon nivale*, comb. nov., yet another crustose species in the genus. *Bryologist* **106:** 565–568.

Gardes, M. & Bruns, T. D. (1993) ITS primers with enhanced specificity for basidiomycetes – application to the identification of mycorrhizae and rusts. *Molecular Ecology* **2:** 113–118.

Goloboff, P. A. (1999) Analyzing large data sets in reasonable times: solutions for composite optima. *Cladistics* **15:** 415–428.

Goloboff, P. A., Farris, J. S. & Nixon, K. C. (2008) TNT, a free program for phylogenetic analysis. *Cladistics* **24:** 774–786.

Högnabba, F. (2006) Molecular phylogeny of the genus *Stereocaulon* (*Stereocaulaceae*, lichenized ascomycetes). *Mycological Research* **110:** 1080–1092.

Huelsenbeck, J. & Roquist, F. (2001) MRBAYES: Bayesian inference of phylogenetic trees. *Bioinformatics* **17**: 754–755.

Jahns, H. M. (1970) Untersuchungen zur Entwicklungsgeschichte der Cladoniaceen unter besonderer Berücksichtigung des Podetien-Problems. *Nova Hedwigia* **20:** 1–177.

Jahns, H. M., Klöckner, P., Jørgensen, P. M. & Ott, S. (1995) Development of thallus and ascocarps in *Stereocaulon tornense*. *Bibliotheca Lichenologica* **58:** 181–190.

Jørgensen, P. M. & Jahns, H. M. (1987) *Muhria*, a remarkable new lichen genus from Scandinavia. *Notes from the Royal Botanic Garden Edinburgh* **44:** 581–599.

Lamb, I. M. (1951) On the morphology, phylogeny, and taxonomy of the lichen genus *Stereocaulon*. *Canadian Journal of Botany* **29:** 522–584.

Lamb, I. M. (1977) A conspectus of the lichen genus *Stereocaulon* (Schreb.) Hoffm. *Journal of the Hattori Botanical Laboratory* **43:** 191–355.

Lohtander, K., Myllys, L., Sundin, R., Källersjö, M. & Tehler, A. (1998) The species pair concept in the lichen *Dendrographa leucophaea* (*Arthoniales*): analyses based on ITS sequences. *Bryologist* **101:** 404–411.

Lumbsch, H. T. & Huhndorf, S. M. (2010) Myconet Volume 14. Part One. Outline of Ascomycota–2009. Part Two. Notes on Ascomycete Systematics. Nos. 4751–5113. *Fieldiana: Life and Earth Sciences* **1:** 1–64.

Lutzoni, F., Kauff, F., Cox, C., McLaughlin, D., Celio, G., Dentinger, B., Padamsee, M., Hibbett, D., James, T. Y., Baloch, E. *et al.* (2004) Assembling the fungal tree of life: progress, classification, and evolution of subcellular traits. *American Journal of Botany* **91:** 1446–1480.

Maddison, D. R. & Maddison, W. P. (2003) *MacClade 4: Analysis of Phylogeny and Character Evolution*. Version 4.06. Sunderland, Massachusetts: Sinauer Associates.

Maddison, W. P. & Maddison, D. R. (2010) *Mesquite: a modular system for evolutionary analysis*. Version 2.73. http://mesquiteproject.org

Miądlikowska, J., Kauff, F., Hofstetter, V., Fraker, E., Grube, M., Hafellner, J., Reeb, V., Hodkinson, B. P., Kukwa, M., Lücking, R. *et al.* (2006) New insights into classification and evolution of the Lecanoromycetes (Pezizomycotina, Ascomycota) from phylogenetic analyses of three ribosomal RNA- and two protein-coding genes. *Mycologia* **98:** 1088–1103.

Myllys, L., Lohtander, K., Källersjö, M. & Tehler, A. (1999) Sequence insertions and ITS data provide congruent information on *Roccella canariensis* and *R. tuberculata* (*Arthoniales*, Euascomycetes) phylogeny. *Molecular Phylogenetics and Evolution* **12:** 295–309.

Myllys, L., Lohtander, K. & Tehler, A. (2001) *β*-tubulin, ITS and group I intron sequences challenge the species pair concept in *Physcia aipolia* and *P. caesia*. *Mycologia* **93:** 335–343.

Myllys, L., Högnabba, F., Lohtander, K., Thell, A., Stenroos, S. & Hyvönen, J. (2005) Phylogenetic relationships of *Stereocaulaceae* based on simultaneous analysis of beta-tubulin, GAPDH and SSU rDNA sequences. *Taxon* **54:** 605–618.

Nixon, K. C. (1999) The parsimony ratchet, a new method for rapid parsimony analysis. *Cladistics* **15:** 407–414.

Nylander, J. A. A. (2004) *MrModelTest 2.1*. Program distributed by the author. Evolutionary Biology Centre, Uppsala University. Available at http://www.abc.se/~nylander.

Orange, A., James, P. W. & White, F. J. (2001) *Microchemical Methods for the Identification of Lichens*. London: British Lichen Society.

Printzen, C. & Kantvilas, G. (2004) *Hertelidea*, genus novum Stereocaulacearum (Ascomycetes lichensiati). *Bibliotheca Lichenologica* **88:** 539–553.

Purvis, O. W. & James, P. W. (1985) Lichens of the Coniston copper mines. *Lichenologist* **17:** 221–237.

Rambaut, A. (2009) *FigTree. Version 1.3.1*. Institute of Evolutionary Biology, University of Edinburgh. http://tree.bio.ed.ac.uk/software/figtree

Rambaut, A. & Drummond, A. J. (2007) *Tracer version 1.4*. http://beast.bio.ed.ac.uk/Tracer.

Stamatakis, A. (2006) RAxML-VI-HPC: maximum likelihood-based phylogenetic analyses with thousands of taxa and mixed models. *Bioinformatics* **22:** 2688–2690.

Timdal, E. (2002) *Stereocaulon cumulatum* comb. nov., another crustose species in the genus. *Lichenologist* **34:** 7–11.

Varón, A., Vinh, L. S., Bomash, I. & Wheeler, W. C. (2008) *POY 4.1.2.1*. American Museum of Natural History, New York. Documentation by Varón, A., Vinh, L. S., Bomash, I., Wheeler, W. C., Tëmkin, I., Cevasco, M., Pickett, K. M., Faivovich, J., Grant, T. & Smith, W. L. http://research.amnh.org/scicomp/projects/poy.php and http://code.google.com/p/poy4/

Varón, A., Vinh, L. S. & Wheeler, W. C. (2010) POY version 4: phylogenetic analysis using dynamic homologies. *Cladistics* **26:** 72–85.

Wheeler, W. C. (1996) Optimization alignment: the end of multiple sequence alignment in phylogenetics? *Cladistics* **12:** 1–9.

White, T. J., Bruns, T., Lee, S. B. & Taylor, J. W. (1990) Amplification and direct sequencing of fungal ribosomal RNA genes for phylogenetics. In *PCR Protocols: A Guide to Methods and Applications* (M. A. Innis, D. H. Gelfand, J. J. Sninsky & T. J. White, eds): 315–322. San Diego: Academic Press.

Appendix 1. Search options used in the POY analysis. For explanations of the commands see Varón *et al.* (2008).

The following commands were used in the direct optimization analysis:

```
read("CrustSter28its1.fas","CrustSter28its3.fas","CrustSter28BTint.fas")
read(prealigned:("CrustSter28its2.fas",tcm:"111.txt"))
read(prealigned:("CrustSter28bt1.fas",tcm:"111.txt"))
read(prealigned:("CrustSter28bt2.fas",tcm:"111.txt"))
set(seed:1,log:"CrustSter28.log",root:"LeprolomamembranaceumMandL272")
transform((all,tcm:"111.txt"))
build(1000)
swap(threshold:10)
select()
perturb(transform(static_approx),iterations:15,ratchet:(0.2,3))
select()
fuse(iterations:200,swap())
select()
report(asciitrees)
report("CrustSter28graphtrees",graphtrees)
report("CrustSter28graphstrictconsensus",graphconsensus)
report("CrustSter28trees.txt",trees)
report("CrustSter28strictconsensus.txt",consensus)
report("CrustSter28stats.txt",treestats)
report("CrustSter28impliedalignment",ia:names:("CrustSter28its1.fas",
  "CrustSter28its3.fas","CrustSter28BTint.fas"))
report("CrustSter28.time",timer:"total time")
set(nolog)
exit()
```